

## Indirect Determination of Water and Hydrogen Peroxide Oxidation by Oxygen Evolution Studies using Multiwalled Carbon Nanotube-Nickel Oxide film as Electrocatalyst

Binesh Unnikrishnan, Yogeswaran Umasankar<sup>‡</sup>, Shen-Ming Chen<sup>\*</sup>, Chien-Chieh Ti

Department of Chemical Engineering and Biotechnology, National Taipei University of Technology, No.1, Section 3, Chung-Hsiao East Road, Taipei 106, Taiwan (R.O.C).

\*E-mail: [smchen78@ms15.hinet.net](mailto:smchen78@ms15.hinet.net)

<sup>‡</sup> Present address: Nanoscale Science and Engineering Center and Faculty of Engineering, University of Georgia, Athens, Georgia 30602, United States.

Received: 19 February 2012 / Accepted: 13 March 2012 / Published: 1 April 2012

---

An electroactive composite film (MWCNT-NiOx) containing multi-walled carbon nanotubes (MWCNTs) with nickel oxide (NiOx) was synthesized on glassy carbon electrode, gold and indium tin oxide (ITO) by cyclic voltammetry (CV). The surface morphology of the composite films deposited on transparent semiconductor ITO was studied using scanning electron microscopy and atomic force microscopy. The quantity and the rate of NiOx deposition on bare and MWCNT modified electrodes were studied using electrochemical quartz crystal microbalance (EQCM). The EQCM results showed that MWCNT catalyses NiOx electrodeposition. Further, the CV studies also proved the presence of MWCNTs in the composite film enhanced the surface coverage concentration of NiOx. The MWCNT-NiOx film showed characteristic voltammetric peaks of Ni<sup>II/III</sup> redox couple. However, the reversibility, i.e., the electrocatalytic activity of Ni<sup>II/III</sup> entirely depends on pH of the electrolyte. The optimized pH range for good electrocatalytic activity was found to be pH 9 to 13. MWCNT-NiOx composite film can catalyze the oxidation of water and hydrogen peroxide with the evolution of oxygen, where the evolved oxygen is detected using the same composite film. Therefore, the determination of H<sub>2</sub>O and H<sub>2</sub>O<sub>2</sub> oxidation has been done indirectly by measuring the evolved oxygen at MWCNT-NiOx by CV.

---

**Keywords:** Multi-walled carbon nanotube, NiOx, O<sub>2</sub> reduction, electrocatalysis, H<sub>2</sub>O, H<sub>2</sub>O<sub>2</sub>, oxygen evolution, water oxidation, electrochemistry.

### 1. INTRODUCTION

Electrodeposition is a simple but powerful method helpful in targeting for selective modification of different types of electrodes with desired matrices. Electroactive metal oxides and carbon nanotube (CNT) matrices have received considerable attraction in recent years because of their

unique chemical, mechanical, electrical, and electrochemical properties. On the other hand a wide variety of applications of matrices made of CNTs for the detection of bioorganic and inorganic compounds such as insulin, ascorbic acid, etc., were already reported in the literature [1-4]. Even though the electrocatalytic activity of the metal oxides and CNTs individually showed good results; some properties like mechanical stability, sensitivity for different techniques and electrocatalysis for multiple compound detections were poor. To overcome this, new studies were developed in the past decade for the preparation of the composite films composed of both CNTs and metal oxides. The rolled-up graphene sheets of carbon exhibits a  $\pi$ -conjugative structure with a highly hydrophobic surface. This unique property of the CNTs allows them to interact with some organic aromatic compounds through  $\pi$ - $\pi$  electronic and hydrophobic interactions and forms new structures [5-7]. Past attempts have been made for preparing composite and sandwiched films made of polymer adsorbed on CNTs and using it for electrocatalytic studies such as selective detection of dopamine in presence of ascorbic acid [8]. The sandwiched films had also used in the designing of nano devices with the help of non-covalent adsorption, electrodeposition, etc. [9, 10]. Electrodes modified with composite films were widely used in capacitors, battery and material science, photo electrochemistry, fuel cells, chemical sensors and biosensors [11, 12].

Nickel oxide (NiOx) is a cheap and easily available material and also easy for processing. In alkaline media NiOx acquires electroactive properties due to the formation of Ni(OH)<sub>2</sub>/NiOOH redox centers [13]. NiOx and nickel hexacyanoferrate modified electrodes have been widely studied for their interesting electrochemical applications [14-16]. NiOx shows good electrocatalytic properties towards some organic compounds like glucose [17, 18], aliphatic alcohols [19, 20], polyhydroxyl compounds [21], oxidation of sulphide [22], aspirin [23], some pharmaceutical drugs [24] etc., in alkaline media. Further, NiOx can catalyze oxygen evolution reactions [25-27]. Therefore several methods have been adopted for electrode modification by NiOx. NiOx can be electrodeposited on electrode surface by potentiostatic, potential cycling or galvanostatic method followed by heat treatment [28]. Sonavane *et al.*, deposited NiOx thin films on fluoride doped tin oxide electrodes by cathodic electrodeposition method without post heat treatment [29] from nickel chloride solutions. However, severe cracks were observed as the deposition time was increased and the thin film was not porous, which is not attractive for biosensor applications. In this paper, we report the electroactive film (MWCNTs-NiOx) made of multiwalled carbon nanotubes (MWCNTs) with NiOx, its characterization and its enhancement in functional properties, peak current and electrocatalytic activity towards H<sub>2</sub>O and H<sub>2</sub>O<sub>2</sub>. The film fabrication process involves the modification of glassy carbon electrode (GCE) with uniform well dispersed MWCNTs and then electrodeposition of the NiOx from neutral aqueous solution on the MWCNTs modified GCE.

## 2. EXPERIMENTAL

### 2.1. Materials

NiCl<sub>3</sub>.6H<sub>2</sub>O, MWCNT (OD = 10-20 nm, ID = 2-10 nm and length = 0.5-200  $\mu$ m), KOH and H<sub>2</sub>O<sub>2</sub> were obtained from Aldrich and Sigma-Aldrich were used as received. All other chemicals used

were of analytical grade. The preparation of aqueous solution was done with twice distilled deionized water. Solutions were deoxygenated by purging with pre-purified nitrogen gas. The pH 9.0 aqueous buffer solution was prepared from 0.025 M  $\text{Na}_2\text{B}_4\text{O}_7 \cdot 10\text{H}_2\text{O}$  with 0.1 M NaOH in the ratio of 55:1. The pH 13 aqueous solution was prepared from 0.1 M KOH.

## 2.2. Apparatus

Cyclic voltammetry (CV) was performed in an analytical system model CHI-611 and CHI-750A potentiostat. A conventional three-electrode cell assembly consisting of an Ag/AgCl reference electrode and a Pt wire counter electrode were used for the electrochemical measurements. The working electrode was either an unmodified GCE or a GCE modified with the NiOx, MWCNTs or MWCNTs-NiOx composite films. In these experiments, all the potentials were reported versus the Ag/AgCl reference electrode. The working electrode for electrochemical quartz crystal microbalance (EQCM) measurements was an 8 MHz AT-cut quartz crystal coated with a gold electrode. The diameter of the quartz crystal was 13.7 mm; the gold electrode diameter was 5 mm. The morphological characterizations of the films were examined by scanning electron microscopy (SEM) (Hitachi S-3000H) and Atomic force microscopy (AFM) by Being nano-instruments CSPM 4000. All the measurements were carried out at  $25\text{ }^\circ\text{C} \pm 2$ .

## 2.3. Fabrication of MWCNTs-NiOx composite modified electrodes

There was an important challenge in the preparation of homogeneous dispersion of MWCNT in aqueous solutions due to its hydrophobic property. Therefore, it is essential to induce surface charges or polar functional groups on MWCNT to make it soluble in aqueous media [30-32]. The hydrophobic nature of the MWCNT was converted to hydrophilic nature by following the previous studies [33]. 10 mg of MWCNT and 200 mg of KOH were taken in to a ruby mortar and ground together for 2 h at room temperature. Then the reaction mixture was dissolved in 10 ml of deionized water and precipitated many times in methanol for the removal of KOH. The obtained MWCNT was ultrasonicated in 10 ml water for 6 h to get a uniform dispersion. This process not only converts MWCNT to hydrophilic nature but also helps to breakdown larger bundles of MWCNT in to smaller ones. This was confirmed using SEM studies. Before starting each experiment, the GCEs were polished by a BAS polishing kit with  $0.05\text{ }\mu\text{m}$  alumina slurry, washed, and then ultrasonicated in deionized water. The GCEs studied were uniformly coated with  $5.6\text{ }\mu\text{g cm}^{-2}$  of MWCNT by drop casting and dried at room temperature, and then the NiOx was deposited on the MWCNT modified GCE by the electrochemical deposition from  $\text{NiCl}_3 \cdot 6\text{H}_2\text{O}$  ( $1 \times 10^{-3}\text{ M}$ ) in pH 9.0 aqueous solution. It was performed by consecutive potential cycling by CV over a suitable potential range of 0.3 to 1.1 V. Then, the modified MWCNT-NiOx electrode was carefully washed with deionized water.

### 3. RESULTS AND DISCUSSIONS

#### 3.1. Synthesis and characterization of MWCNT-NiOx composite film

The electrodeposition of NiOx on MWCNT modified GCE was done from  $\text{NiCl}_3 \cdot 6\text{H}_2\text{O}$  ( $1 \times 10^{-3}$  M) in pH 9.0 aqueous solution by continuous potential cycling by CV for 10 cycles.

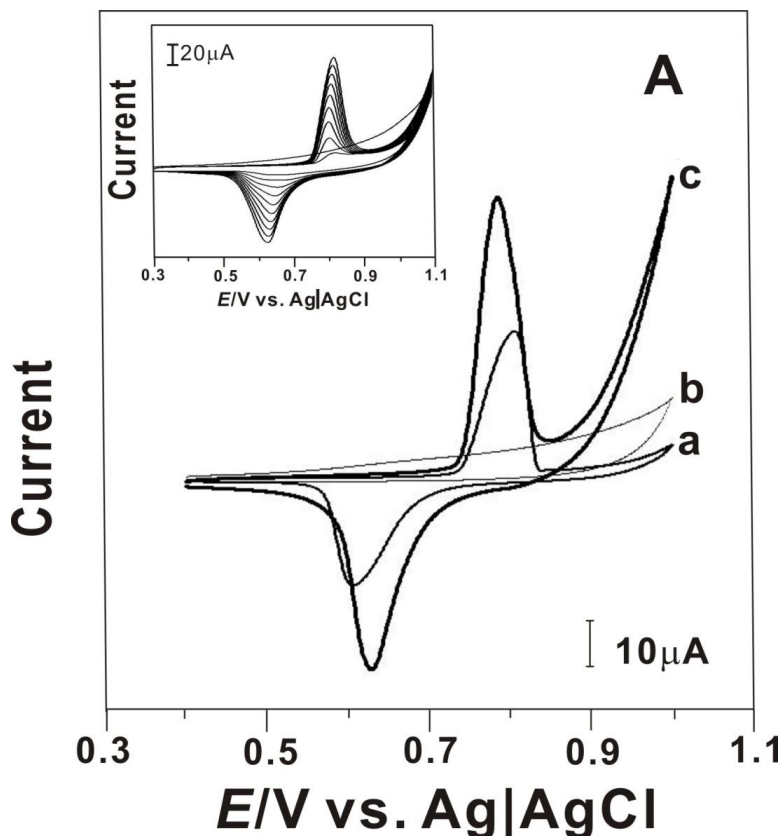


**Figure 1.** Cyclic voltammograms of (a) NiOx, (b) MWCNT, (c) MWCNT- NiOx modified GCE in pH 9 at a scan rate of  $100 \text{ mVs}^{-1}$ . Inset shows the cyclic voltammogram of NiOx electrodeposition on GCE/MWCNT in pH 9 containing  $1 \times 10^{-3}$  M  $\text{NiCl}_3 \cdot 6\text{H}_2\text{O}$ ; scan rate of  $100 \text{ mVs}^{-1}$ . Potential range: 0.3 to 1.1 V.

Inset in Fig. 1 represents the electrodeposition of NiOx on the MWCNT modified GCE with redox peaks correspond to the formation of NiOx ( $\text{Ni}^{\text{III/II}}$ ) with formal potential  $E^{\circ'} = 0.70$  V versus Ag/AgCl. The NiOx is deposited by the oxidation of the  $\text{Ni}^{2+}$  to  $\text{Ni}^{3+}$  and undergoes oxidation and reduction during the potential cycling to form hydrated oxides [34]. During the first potential cycle no anodic peak appears and during the reverse scan a small and broad cathodic peak appears at around 0.62 V due to the reduction of  $\text{Ni}^{3+}$  at the electrode surface. Then, from second cycle onwards the anodic peak grows significantly. The redox peaks grow further on subsequent cycles which indicates the building up of NiOx on MWCNT modified GCE. Peng *et al.*, [35] synthesized polyaniline-NiOx composite by co-deposition using cyclic voltammetry in pH 7.3. In their case, during the electrodeposition of NiOx, the anodic peak initially appeared at about 1.1 V and shifted to 1.2 V in the subsequent potential cycles. However, in this work no significant peak potential shift is observed

during the growth of NiOx, showing stable deposition. Similarly, NiOx has been electrodeposited on GCE for comparison. The NiOx modified electrodes have been washed and dried, and then their electrochemical behavior has been studied by CV. The cyclic voltammograms of GCE/NiOx, GCE/MWCNT and GCE/MWCNT-NiOx in pH 9.0 are given in Fig. 1. For GCE/MWCNT-NiOx the redox peaks appear with the anodic peak at 0.78 V and the cathodic peak at about 0.63V with  $\Delta E_p$  value of 0.15 V. The GCE/MWCNT-NiOx shows higher anodic ( $I_{pa}$ ) and cathodic peak currents ( $I_{pc}$ ) and lower  $\Delta E_p$  value than GCE/NiOx indicating the compatibility of the MWCNT matrix for NiOx deposition. Assuming one electron transfer [27] involved for  $Ni^{III/II}$  in pH 9.0 the surface coverage concentration ( $\Gamma$ ) of NiOx on bare GCE and GCE/MWCNT have been calculated from the equation  $\Gamma = Q/nfA$ . Where,  $Q$  is the charge,  $n$  is the number of electrons,  $f$  is the Faraday constant and  $A$  is the area of the electrode. At bare GCE the NiOx surface coverage is  $7.96 \times 10^{-9}$  mol  $cm^{-2}$  whereas, at GCE/MWCT it is  $1.04 \times 10^{-8}$  mol  $cm^{-2}$ . This observation indicates that MWCNT increases the surface area of the electrode, which in turn increases the  $\Gamma$  of NiOx. In all the following experiments, each newly prepared composite film on GCE was washed carefully in deionized water to remove any loosely adsorbed  $NiCl_3 \cdot 6H_2O$ , and then transferred to pH 9.0 aqueous solution for the electrochemical characterizations.

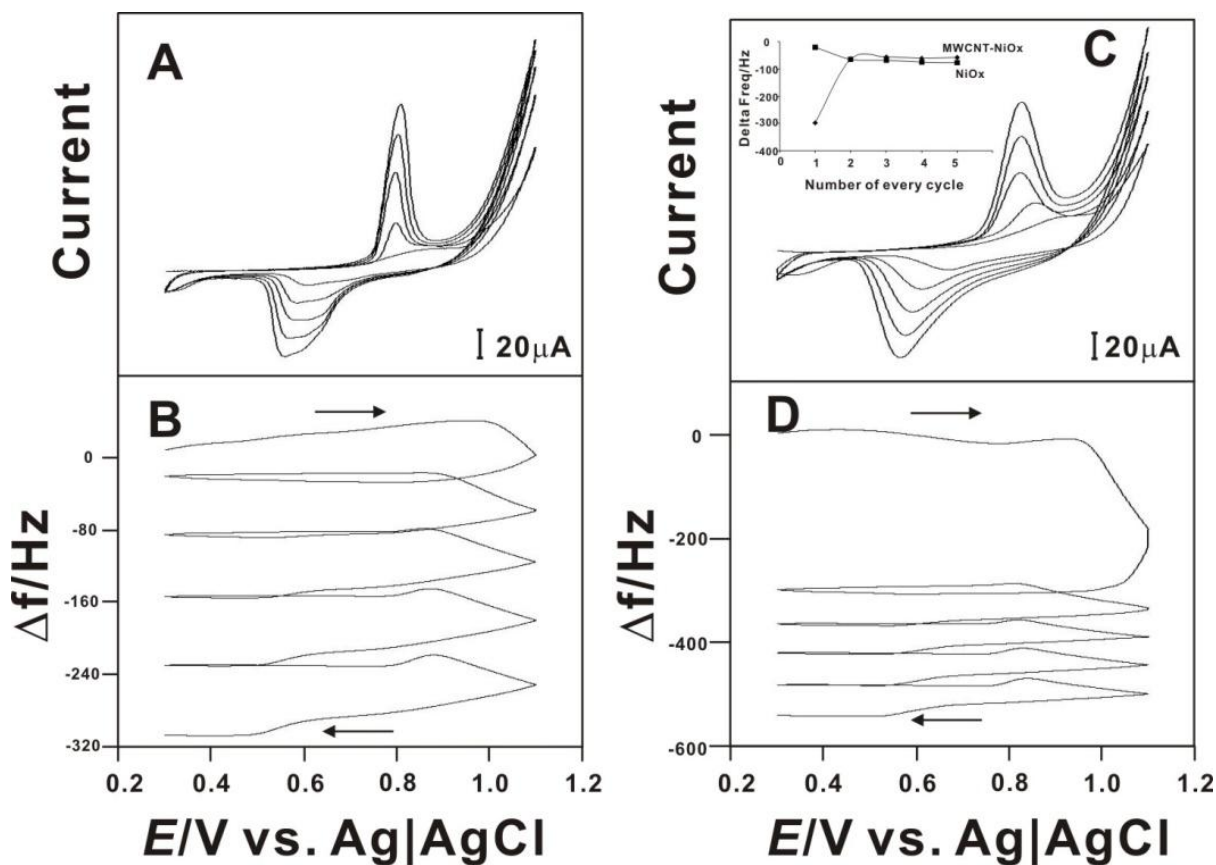


**Figure 2.** (A) and (C) 5 consecutive cyclic voltammograms of GCE/MWCNT and bare GCE, respectively, in pH 9.0 containing  $1 \times 10^{-3}$  M  $NiCl_3 \cdot 6H_2O$ . Scan rate =  $100 \text{ mVs}^{-1}$ . (B) and (D): The corresponding EQCM frequency change observed for 5 consecutive cyclic voltammograms of (A) and (C) respectively. Inset to (C) is the number of cycle vs.  $\Delta\text{Hz}$  for each cycle.

EQCM experiments were carried out by modifying the gold electrode in electrochemical quartz crystal with uniformly coated  $1.8 \mu\text{g cm}^{-2}$  MWCNT. The consecutive potential cycling and EQCM measurements for NiOx deposition were done in pH 9.0 aqueous solution containing  $1 \times 10^{-3}$  M  $\text{NiCl}_3 \cdot 6\text{H}_2\text{O}$ . The increase in  $I_{\text{pa}}$  and  $I_{\text{pc}}$  of NiOx redox couple and the decrease in frequency (or increase in mass) were found to be consistent with the growth of the NiOx film on MWCNT modified Au electrode. Similarly, the consecutive cyclic voltammograms and EQCM measurements were also recorded for the NiOx deposition on Au electrode of the quartz crystal with the same experimental conditions, for comparison. Fig. 2(A) and (C) represent the cyclic voltammograms of electrodeposition of NiOx on bare Au and MWCNT modified Au electrode, respectively. Fig. 2 (B) and (D) are the respective diagrams for the frequency change ( $\Delta\text{Hz}$ ) during the consecutive potential cycling. These results show that the obvious deposition potential is between 0.3 and 1.1 V. Inset to Fig. 2(C) indicates the plot of number of cycles vs.  $\Delta\text{Hz}$  for each cycle.

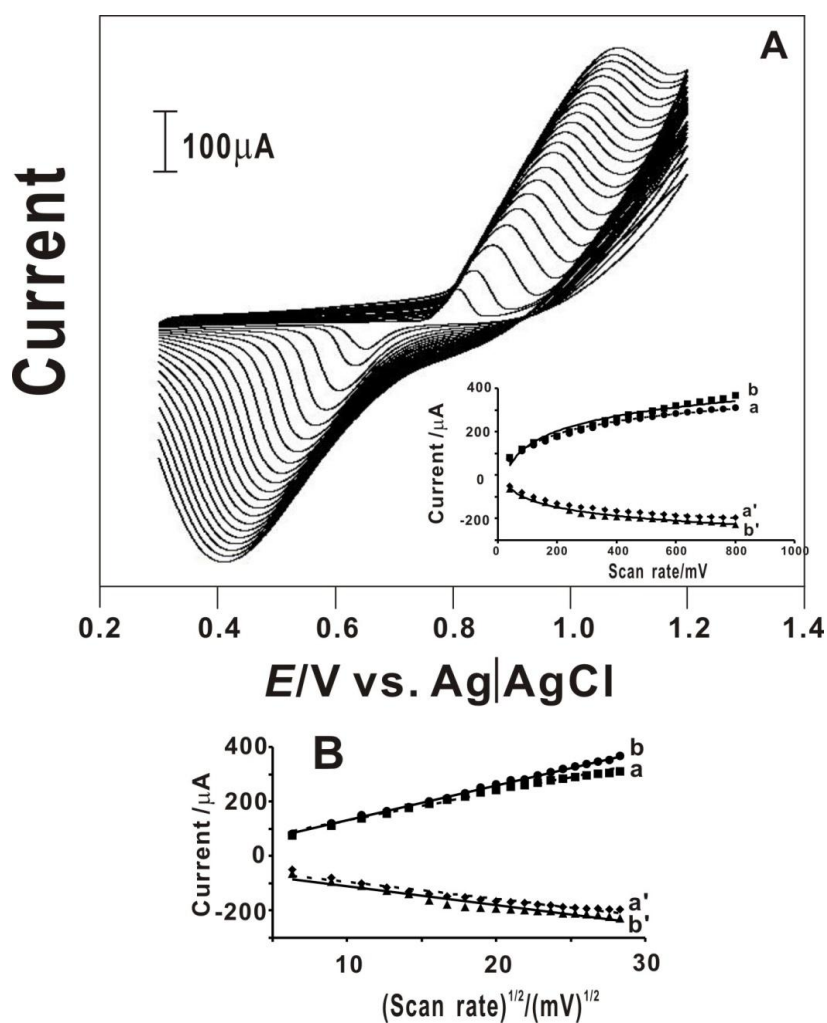


**Figure 3.** (A) Cyclic voltammograms of MWCNT-NiOx film at GCE in pH 9 at various scan rates from inner to outer are: 40 to 800  $\text{mVs}^{-1}$ . Inset of (A) is the plot of scan rate vs. peak current. (B) is  $(\text{scan rate})^{1/2}$  vs. peak current. a is the  $I_{\text{pc}}$  and a' is the  $I_{\text{pa}}$  of NiOx on bare GCE; and b is the  $I_{\text{pc}}$  and b' is  $I_{\text{pa}}$  of GCE/MWCNT-NiOx.

At MWCNT modified Au, the rate of frequency change is larger than that of bare Au during the first cycle and it become uniform for the subsequent potential cycle. Au electrode also shows almost same rate of  $\Delta\text{Hz}$  for every potential cycle. From the  $\Delta\text{Hz}$  values, the change in the mass of composite film at the quartz crystal can be calculated by the Sauerbery equation, and it is found that 1 Hz frequency change is equivalent to 1.4 ng of mass change [36, 37]. Thus, the mass change during NiOx electrodeposition on the bare Au and MWCNT modified Au for 5 cycles are 428 ng  $\text{cm}^{-2}$  and 831 ng  $\text{cm}^{-2}$  respectively. These results indicate the MWCNT acts as a stable host for stable NiOx film.

The effect of the scan rate ( $\nu$ ) on the redox behavior of the NiOx film has been studied in pH 9.0. The cyclic voltammograms of GCE/MWCNT-NiOx were recorded at different scan rates in the range of 40-800  $\text{mVs}^{-1}$ . Both the  $I_{\text{pa}}$  and  $I_{\text{pc}}$  of  $\text{Ni}^{\text{III/II}}$  redox couple increase with the increase in scan rates up to 800  $\text{mV s}^{-1}$  as shown in Fig. 3(A). The ratio of  $I_{\text{pa}}/I_{\text{pc}}$  remained almost unity; however,  $I_{\text{pc}}$  and  $I_{\text{pa}}$  do not show linear relationship with the increase in scan rate (peak current vs.  $\nu$ ) as shown in the inset of Fig. 3(A). And, the plot of peak current vs.  $\nu^{1/2}$  (Fig. 3(B)) shows a linear relationship in the entire range of scan rate. These results suggest that the redox processes of NiOx in pH 9.0 at MWCNT modified GCE is diffusion controlled electrode process. Similar behavior has been reported for NiOx in alkaline media [38].

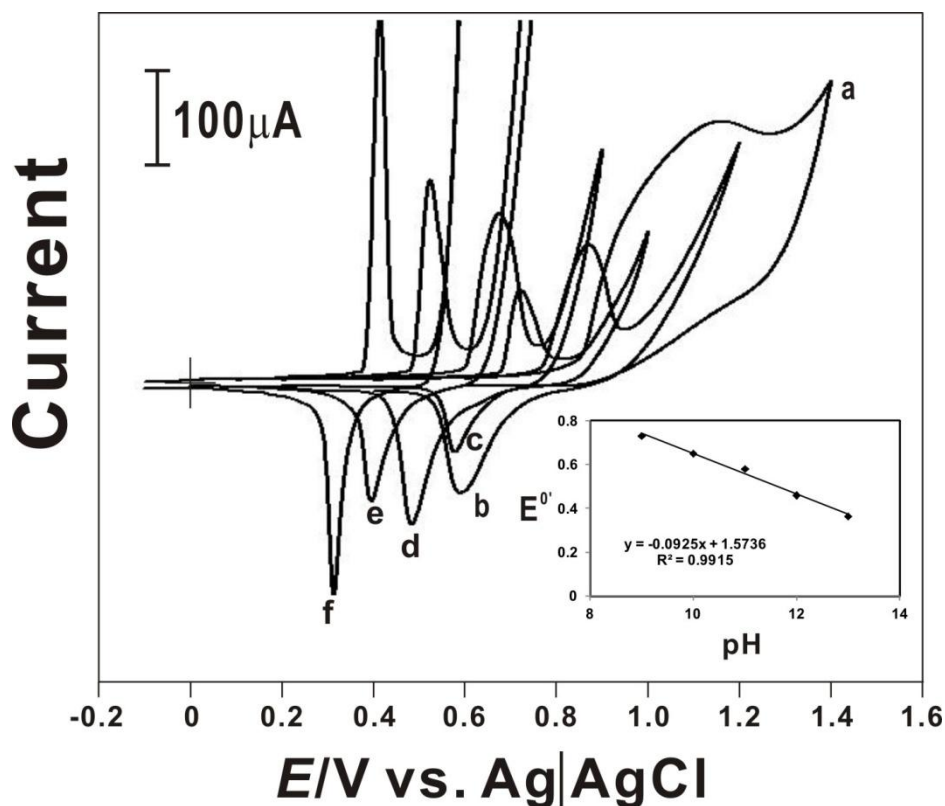


**Figure 4.** Cyclic voltammograms of GCE/MWCNT-NiOx in different pH (a) 8, (b) 9, (c) 10, (d) 11, (e) 12, and (f) 13. Inset: relationship between  $E^{\circ'}$  and pH. Scan rate: 100  $\text{mVs}^{-1}$ .

To understand the effect of pH on the MWCNT-NiOx redox signal, cyclic voltammograms were recorded in various pH (8-13) aqueous solutions at a scan rate of 0.1  $\text{Vs}^{-1}$  and the results are given

in Fig. 4. The MWCNT-NiOx composite film shows redox peaks in pH from 9 to 13 and therefore the film is highly stable in the pH range between 9 and 13. The  $I_{pa}$  and  $I_{pc}$  decrease when the pH is changed from 13 to 9 and the  $\Delta E$  increased. This result indicates decrease in the electroactive sites due to the decrease in the concentration of  $\text{OH}^-$  ions in lower pH solutions [39]. Both  $E_{pc}$  and  $E_{pa}$  are dependent on pH and shift towards more negative potential region with the increase in pH. Also, it can be seen from the figure that as the pH increases, the electrode process acquires more reversible character. Therefore, it suggests that a higher pH will be more favorable for the performance of MWCNT-NiOx composite film for electrochemical applications. The inset of Fig. 4 shows the plot of formal potential as a function of pH in the range of 9 to 13.

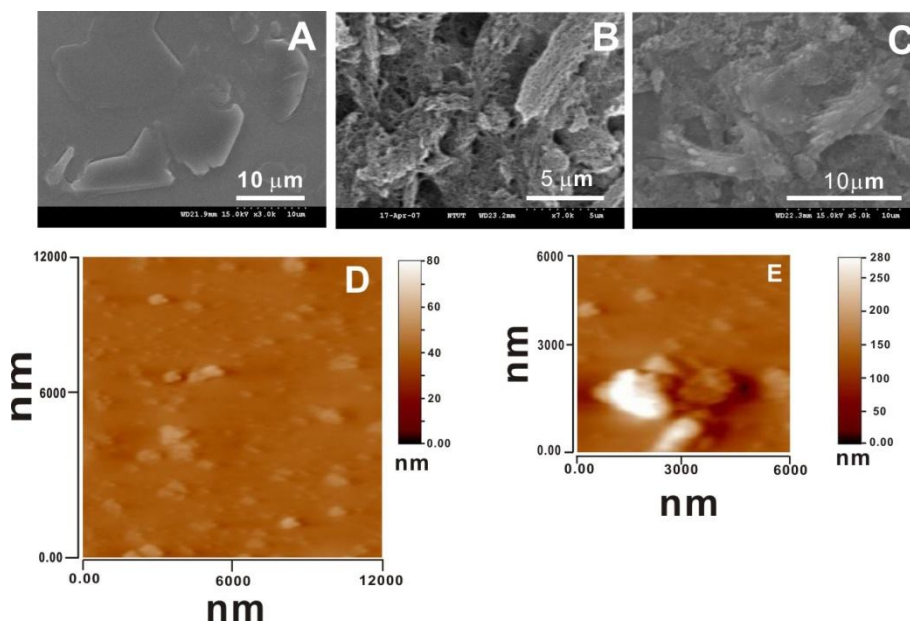


**Figure 5.** SEM images of ITO electrode modified with (A) only NiOx, (B) only MWCNT, (C) MWCNT-NiOx and AFM images of ITO electrode modified with (D) only NiOx, and (E) MWCNT- NiOx.

The surface morphology of different films has been studied by SEM and AFM. MWCNT, NiOx and MWCNT-NiOx composite films were prepared on indium tin oxide (ITO) with the same conditions mentioned in section 2.3. Fig. 5 shows the SEM and AFM images of various films covering the ITO surface. From Fig. 5, it can be seen that there are morphological differences among all these films. NiOx deposited on bare GCE exhibits agglomerated large particle like structures (A) and MWCNT (B) appears as large mass of nano fibers with porous structures. Fig. 5(C) shows a slightly different surface morphology with NiOx deposited on MWCNT forming a composite. When comparing all the images, it is obvious that the deposition of NiOx took place on MWCNT modified ITO. Similarly, the AFM topography studies have been done for the modified ITO electrodes and the images are shown in Fig. 5(D) NiOx and (E) MWCNT-NiOx. MWCNT-NiOx composite film has a thickness of about 280 nm. The observed morphological structures show significant difference as expected.

3.2. Electrochemical oxidation of H<sub>2</sub>O and H<sub>2</sub>O<sub>2</sub> at MWCNTs-NiOx composite film

Fig. 6 shows the electrochemical oxidation of H<sub>2</sub>O by CV in pH 13.0 aqueous solution. The solution was deoxygenated by purging purified nitrogen gas for 20 min prior to the experiment.

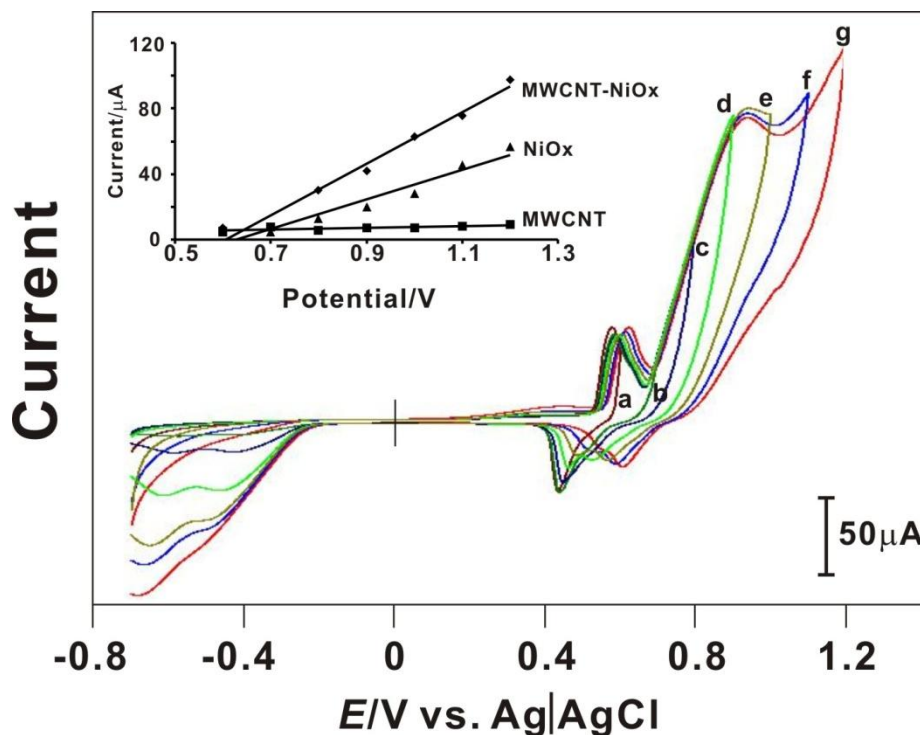
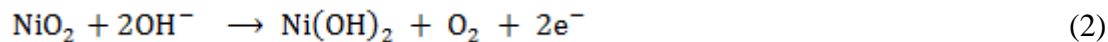


**Figure 6.** Effect of switching potentials on oxidation of H<sub>2</sub>O and on O<sub>2</sub> evolution at MWCNT-NiOx film in pH 13 aqueous solution between -0.8 V and a) 0.6, b) 0.7, c) 0.8, d) 0.9, e) 1.0, f) 1.1 and g) 1.2 V. Inset shows  $I_{pc}$  of [O<sub>2</sub>] vs. switching potentials of MWCNT-NiOx, NiOx and MWCNT films.

Then, CVs were recorded at constant time interval without nitrogen purging at a scan rate of 20 mV s<sup>-1</sup>. The cyclic voltammograms of the MWCNT-NiOx showed in Fig. 6 exhibit a redox couple for Ni<sup>III/II</sup> during the potential scan from -0.8 to 0.6 V. When the scanning potential range is increased towards more positive side (0.7 to 1.2 V), a shift in the redox peaks towards more positive potential is observed and a new reduction peak is appeared at -0.4 and -0.6 V. Further, the new peak increases with increase in the potential range. These results show that there is an increase in concentration of O<sub>2</sub> when increasing the scanning range. The shift in potential of the Ni<sup>III/II</sup> redox peak and the increase in concentration of the oxygen can be explained as a complex reaction of water oxidation and Ni<sup>IV</sup> formation. Removal of a proton from a hydroxyl group bonded to Ni<sup>3+</sup> ion requires less energy than a hydroxyl group bonded to a Ni<sup>2+</sup> ion [40] and therefore the kinetic factors favor the formation of Ni<sup>IV</sup>. A significant quantity of Ni<sup>IV</sup> is produced during the anodic process [41, 42] which can be represented as given in equation (1).



The as-formed NiO<sub>2</sub> is unstable [43] and decomposes to give O<sub>2</sub> which can be represented as given in equation 2.



The inset in Fig. 6, potential vs. peak current at -0.6 V shows the comparison of peak currents obtained for oxygen reduction at MWCNT-NiOx, NiOx, and MWCNT film modified electrodes, where the MWCNT-NiOx show higher oxygen reduction [44] current than other two films. This enhancement in the reduction of oxygen can be attributed to more oxygen evolution due to the increase in water oxidation in MWCNT-NiOx compared to other two electrodes.

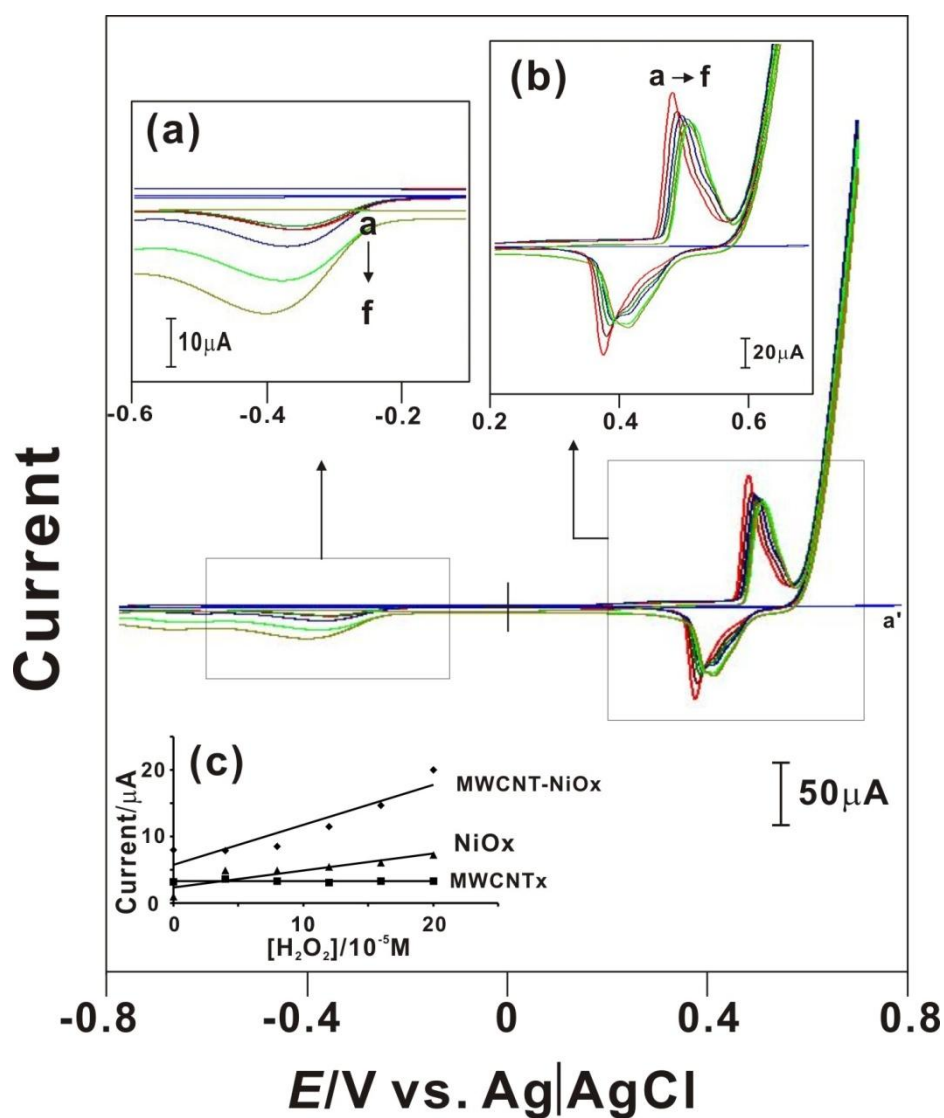


**Figure 7.** Cyclic voltammograms of MWCNT-NiOx film in pH 13 solution containing different concentrations of [H<sub>2</sub>O<sub>2</sub>]; a) 0.0, b) 4 × 10<sup>-5</sup> M, c) 8 × 10<sup>-5</sup> M, d) 12 × 10<sup>-4</sup> M, e) 16 × 10<sup>-5</sup> M, and f) 20 × 10<sup>-5</sup> M. (a') bare GCE and [H<sub>2</sub>O<sub>2</sub>] = 20 × 10<sup>-5</sup> M. Inset shows *I*<sub>pc</sub> vs. different concentrations of [H<sub>2</sub>O<sub>2</sub>] at MWCNT-NiOx, NiOx and MWCNT films.

The electrocatalysis of  $\text{H}_2\text{O}_2$  at MWCNT-NiOx has been done with the same experimental conditions as that of oxidation of  $\text{H}_2\text{O}$  mentioned above. As can be seen from Fig. 7 that an increase in concentration of  $\text{H}_2\text{O}_2$  simultaneously produced a linear increase in the reduction peak currents of the  $\text{O}_2$  at -0.4 and -0.6 V. An enlarged view of the reduction peak current is given in the inset (a) of Fig. 7. Also, the increase in  $\text{H}_2\text{O}_2$  increases the formal potential of the  $\text{Ni}^{\text{III/II}}$  peak towards the more positive potential (enlarged view is given in inset (b) of Fig. 7).  $\text{H}_2\text{O}_2$  oxidation takes place after the complete oxidation of  $\text{Ni}(\text{OH})_2$  to  $\text{NiOOH}$  and the mechanism of electrochemical oxidation produces  $\text{O}_2$  [38] as given in the equations (3) and (4).



The inset (c) to Fig. 7 shows the linear dependence of the concentration of  $\text{H}_2\text{O}_2$  with the reduction peak current at -0.4 V of various films. In these results too the comparison of peak currents obtained for oxygen reduction at MWCNT-NiOx, NiOx, and MWCNT films shows MWCNT-NiOx has higher oxygen reduction current than other two films. This enhancement in the reduction of oxygen can be attributed to more oxygen evolution due to the increase in  $\text{H}_2\text{O}_2$  oxidation in MWCNT-NiOx compared to other two electrodes.

#### 4. CONCLUSIONS

We demonstrated the preparation of composite material with MWCNTs and NiOx (MWCNTs-NiOx) at the GCE, Au and ITO electrode surfaces by CV. The film showed characteristic redox peaks in aqueous solutions of pH 9 to 13. The indirect determination of  $\text{H}_2\text{O}$  and  $\text{H}_2\text{O}_2$  oxidation process at the MWCNT-NiOx film has been demonstrated by studying the reduction of evolved  $\text{O}_2$ . The developed composite film for the electrocatalysis combines the advantage of ease of fabrication. The EQCM, SEM and AFM results confirmed the deposition of NiOx on MWCNTs modified electrode. The composite film fabricated on GCE and its electrochemical studies presented in this paper provide an opportunity for qualitative and quantitative characterization. Therefore, this work establishes and illustrates, in principle and potential, a simple and novel approach for the development of voltammetric determination based on the MWCNT-NiOx modified GCE.

#### ACKNOWLEDGEMENT

This work was supported by the National Science Council of the Taiwan (R.O.C).

#### References

1. W. Zhang, F. Wan, W. Zhu, H. Xu, X. Ye, R. Cheng and L.T. Jin, *J. of Chromatogr. B.*, 818 (2005) 227.
2. G. Wu, Y. S. Chen and B. Q. Xu, *Electrochem. Commun.*, 7 (2005) 1237.

3. J. Wang and M. Musameh, *Anal. Chim. Acta*, 511 (2004) 33.
4. J. Wang, M. Li, Z. Shi, N. Li and Z. Gu, *Electrochim. Acta*, 47 (2001) 651.
5. Q. Li, J. Zhang, H. Yan, M. He and Z. Liu, *Carbon*, 42 (2004) 287.
6. J. Zhang, J. K. Lee, Y. Wu and R. W. Murray, *Nano Lett.*, 3 (2003) 403.
7. A. Star, T. R. Han, J. Christophe, P. Gabriel, K. Bradley and G. Gruner, *Nano Lett.*, 3 (2003) 1421.
8. M. Zhang, K. Gong, H. Zhang and L. Mao, *Biosens. Bioelectron.*, 20 (2005) 1270.
9. R. J. Chen, Y. Zhang, D. Wang and H. Dai, *J. Am. Chem. Soc.*, 123 (2001) 3838.
10. G. Han, J. Yuan, G. Shi and F. Wei, *Thin Solid Films*, 474 (2005) 64.
11. G. H. Deng, X. Xiao, J. H. Chen, X. B. Zeng, D. L. He and Y. F. Kuang, *Carbon*, 43 (2005) 1557.
12. E. Frackowiak, V. Khomenko, K. Jurewicz, K. Lota and F. Béguin, *J. of Power Sources*, 153 (2006) 413.
13. S. Berchmans, H. Gomathi and G. P. Rao, *J. Electroanal. Chem.*, 394 (1995) 267.
14. S. M. Chen, *J. Electroanal. Chem.*, 417(1996), 145.
15. S. M. Chen, *J. Electroanal. Chem.*, 521(2002), 29.
16. S. M. Chen, C. Y. Liou, R. Thangamuthu, *Electroanalysis*, 19 (2007) 2457.
17. M. Shamsipura, M. Najafi and M. R. M. Hosseini, *Bioelectrochemistry*, 77 (2010) 120.
18. Y. Mua, D. Jia, Y. He, Y. Miao and H. L. Wu, *Biosens. Bioelectron.*, 26 (2011) 2948.
19. I.G. Casella, T. R. I. Cataldi, A. M. Salvi and E. Desimoni, *Anal. Chem.*, 85 (1993) 3143.
20. A.A. E. Shafei, *J. Electroanal. Chem.*, 471 (1999) 89.
21. X. Y. Peng, W. Li, X. X. Liu and P. J. Hua, *J. Appl. Polym. Sci.*, 105 (2007) 2260.
22. D. Giovanelli, N. S. Lawrence and L. Jiang, *Sens. Actuators, B*, 88 (2003) 320.
23. S. Majdi, A. Jabbari and H. Heli, *J. Solid State Electrochem.*, 11 (2007) 1601.
24. A. Salimi, Z. Enferadi, A. Noorbakhash and K. Rashidi, *J. Solid State Electrochem.*, DOI 10.1007/s10008-011-1536-z, (2011).
25. M. E. G. Lyons, and M. P. Brandon, *Int. J. Electrochem. Sci.*, 3 (2008) 1386.
26. G. Bronoel, and J. Reby, *Electrochim. Acta*, 25 (1980) 973.
27. M. F. Kibria, and M. S. Mridha, *Int. J. Hydrogen Energy*, 21 (1996) 179.
28. B. Wen, S. Zhang, H. Fang, W. Liu and Z. Du, *Mater. Chem. Phys.*, 131 (2011) 8-11.
29. A.C. Sonavane, A. I. Inamdar, P. S. Shinde, H. P. Deshmukh, R. S. Patil and P. S. Patil, *J. Alloys Compd.*, 489 (2010) 667.
30. Y. Umasankar, B. Unnikrishnan, S. M. Chen, T. W. Ting, *Int. J. Electrochem. Sci.*, 7 (2012) 484.
31. Y. L. Yang, B. Unnikrishnan, S. M. Chen, *Int. J. Electrochem. Sci.*, 6(2011) 3743.
32. J. W. Shie, U. Yogeswaran, S. M. Chen, *Talanta*, 78(2009) 896.
33. Y. Yan, M. Zhang, K. Gong, L. Su, Z. Guo and L. Mao, *Chem. Mater.*, 17 (2005) 3457.
34. D. Tench, and L. F. Warren, *J. Electrochem. Soc.*, 130 (1983) 869.
35. X. Y. Peng, X. X. Liu and P. J. Hua, *J. Solid State Electrochem.*, 14 (2010) 1.
36. S. M. Chen, and M. I. Liu, *Electrochim. Acta*, 51 (2006) 4744.
37. S. M. Chen, C. J. Liao and V. S. Vasantha, *J. Electroanal. Chem.*, 589 (2006) 15.
38. A. Aytac, M. Gurbuz, A. E. Sanli, *Int. J. Hydrogen Energy*, 36 (2011) 10013.
39. C.C. Hu, and C. Y. Cheng, *J. Power Sources*, 111 (2002) 137.
40. S. A. Aleshkevich, E. I. Golovchenko, V. P. Morozov and L. N. Sagoyan, *Soviet Electrochem.*, 4 (1968) 530.
41. G. W. D. Briggs, Special Periodical Reports in: Electrochemistry, *The Chemical Society*, London, 1974, pp. 33.
42. S. M. Chen, C. H. Wang, *J. Solid State Electrochem.*, 11 (2007) 581.
43. A.J. Motheo, S. A. S. Machado, F. J. B. Rabelo and J. R. Santos Jr., *J. Braz. Chem. Soc.*, 5 (1994) 161.
44. T. H. Tsai, S. H. Wang, S. M. Chen, *Int. J. Electrochem. Sci.*, 6 (2011) 1655.